International Journal of Nanoscience
Vol. 22, No. 2 (2023) 2350015 (7 pages)

DOI: 10.1142/S0219581X23500151



# Studying the Optical and Structural Properties and Anticancer Activity of New PVA–$Fe_2O_3$:Cu Nanocomposite Materials

Amer N. Jarad*, Rawnaq A. Talib*, Ahmed Shayaa Kareem†, Jalal Hasan Mohammed‡, Entidar Jasim Khmees§, Karrar Hazim Salem¶, Rahman S. Zabibah‖, Mohammed Ayad Alkhafaji**, Kahtan A. Mohammed††,§§ and Kuldeep K. Saxena‡‡

*Polymer Research Center,
University of Basrah, Basrah, Iraq*

†Department of Medical Laboratories Techniques,
Imam Ja'afar Al-Sadiq University, Al-Muthanna 66002, Iraq*

‡Faculty of Pharmacy,
University of Kerbala, Kerbala, Iraq*

§Department of Physiology and Medical Physics,
Babylon University, Babylon, Iraq*

¶Pharmacy Department,
Al-Mustaqbal University College, 51001, Hillah, Iraq*

‖Medical Laboratory Technology Department,
College of Medical Technology, The Islamic University
Najaf, Iraq*

**National University of Science and Technology,
Dhi Qar, Iraq*

††Department of Medical Physics,
Hilla University College, Babylon, Iraq*

‡‡Division of Research and Development,
Lovely Professional University, Phagwara 144411, India*

§§Kahtan444@gmail.com*

Received 1 December 2022
Accepted 30 January 2023
Published 9 March 2023

The purpose of this study is to evaluate the structure, morphology and optical properties of a newly developed hybrid structure that was generated from a $Fe_2O_3$–Cu–PVA composite matrix. Several methods, such as field-emission scanning electron microscopy (FESEM), X-ray diffraction (XRD), as well as absorption and transmission spectra, were used to investigate the samples. The addition of copper was found to have no influence on the crystalline arrangement of PVA–$Fe_2O_3$, according to the findings of crystallography. In the wavelength region from 450 nm to 550 nm, the produced composites exhibit significant absorption. It is essential that the region of shorter wavelengths experiences a steady shift toward the region of maximum

absorption in these composites when copper is included. The transmittance of PVA–$Fe_2O_3$ is over 80% in the region of 600–800 nm, making it an extremely transparent material. Following the addition of 5% by weight of copper to the nanocomposite, the transmittance of the material dropped to 50% within the same range of wavelengths. The synthesized materials were put to use as anti-cancer cells, and they demonstrated a high level of effectiveness in the process of killing tumor cells, particularly the PVA–$Fe_2O_3$–Cu combination.

*Keywords*: Iron oxide; PVA; nanocomposite; doping; anticancer.



## 1. Introduction

The discipline of nanoscience is quickly establishing a reputation for being one of the greatest significant fields of research in current sciences. Nanotechnology is starting to make it possible for researchers, engineers, chemists and medical professionals to work at the cellular and molecular stages, which will lead to significant breakthroughs in both life science and health care in the next years. The exploitation of nanoparticle (NP) materials and nanocomposites gives considerable benefits as a result of the one-of-a-kind size and physicochemical characteristics of these particles. These particles can be broken down into extremely small pieces.[1–3]

There are many kinds of NPs, which can be classified according to their size, shape, electrical properties, optical properties and magnetic properties.[4–7]

Researchers throughout the world have taken an intense interest in magnetic nanoparticles (MNPs) due to their utility as models for studying fundamental aspects of magnetic ordering processes in magnetic materials of small dimensions. Discoveries from these investigations can lead to information for the creation of cutting-edge new technologies.[8,9]

Since MNPs are used in biotechnology, healthcare, materials science, engineering and ecological research, their synthesis has gained a lot of attention in recent years.[10]

The properties of MNPs allow for their organization into a few distinct categories, including ferrimagnetic, ferromagnetic and superparamagnetic NPs. As a result of the presence of unpaired electrons, many elements, including iron, manganese and gadolinium, have paramagnetic properties, in addition to elemental MNPs there are compositional MNPs like iron oxides NPs.[11–13]

Iron oxide NPs have been receiving a lot of attention of late due to the unique qualities that they possess. Some of these properties include superparamagnetism, a surface-to-volume ratio, a higher surface area, and a simple separation approach. The synthesis of MNPs with an appropriate surface chemistry has been attempted using a wide variety of physical, chemical and biological approaches.[14]

Hematite (–$Fe_2O_3$), magnetite ($Fe_3O_4$) and maghemite (–$Fe_2O_3$) are the three most common forms of iron oxides that can be discovered in nature. Magnetite is an iron oxide with the formula $Fe_3O_4$. These oxides also play a very important part in the field of scientific study and development.[15,16]

Hematites are minerals that have a hexagonal structure and belong to the category of iron–oxide minerals. They are denoted by the chemical formula $Fe_2O_3$ displaying characteristics of paramagnetic activity. In addition to this, they possess a potent catalytic activity, are extensively dispersed and simple to acquire, and have a very low impact on the surrounding ecosystem. Hematite, in particular, may be a good choice for visible-light photocatalysis since it can absorb visible light, gather up to 45% of the energy in the solar spectrum, and is one of the least expensive semiconductor materials that are currently accessible.[17,18]

$Fe_2O_3$ NPs can be produced by using the chemical method in colloidal form and this form of $Fe_2O_3$ has many applications in a wide range of industries and in medicine.[19–22]

Colloidal $Fe_2O_3$ NPs are considered an important type of nanofluid materials where they can use great thermal properties and heat transfer properties in the industry.[23,24] in addition to their industrial properties colloidal $Fe_2O_3$ NPs having many applications in the medical area.[25,26] The most prominent uses of $Fe_2O_3$ medically are its effectiveness as an antibacterial and in biomedical imaging, and the most important thing is to take advantage of its magnetic properties to treat cancerous tumors.[27–29] Many nanosystems have been used as anticancer agents, Lefojane and his team used $CdO/CdCO_3$ nanocomposites as anticancer materials and the proposed nanosystem shows good activity on tumor cells.[30] The anticancer activity on HepG2

(RCB1648) of NiO nanostructures was also tested by Ayesha Sani *et al.*[31]

Here, in the current work, a new hybrid composite structure has been prepared with an easy method and low-cost raw materials for anticancer applications.

## 2. Experimental Part

### 2.1. *Preparation of PVA–$Fe_2O_3$ nanocomposite*

The details of the production process of PVA–$Fe_2O_3$ nanocomposites have been mentioned in our previous published work.[27,29] PVA polymer was used as capping agent, iron chloride $FeCl_3$ solution was used as Fe ions source, NaOH solution was used as alkaline source; these solutions were mixed on magnetic stirrer to synthesize PVA–$Fe_2O_3$ nanocomposites.

#### 2.1.1. *Preparation of PVA–$Fe_2O_3$ –Cu nanocomposite*

The preparation of PVA–$Fe_2O_3$–Cu nanocomposites follows the same procedure of preparing PVA–$Fe_2O_3$ but with an additional step, which is using 5% mass ratio of copper chloride mixed with iron chloride solution. The rest of the steps are identical to the steps of PVA–$Fe_2O_3$ nanocomposites preparation.

## 3. Results and Discussions

X-ray diffraction had been applied to analyze the crystal structure of the components that had been synthesized. This was done in order to better understand how the materials had been formed. The highest points and most distinctive patterns of the deviation of the newly developed materials are shown in Fig. 1. At an angle of $2\theta = 22°$, one may find a significant peak that corresponds to the PVA polymer. The diffraction points that are connected to $Fe_2O_3$ are able to be observed in a curve. Peaks at The assigned diffractions peaks of $Fe_2O_3$ NPs at the $2\theta$ values of 32.5° (104), 37.9° (110), 47.5° (024), 57.5° (018) and 65.5° (300) are well matched with JCPDS card no. 24-0072 and the same peaks still appeared after preparing the nanocomposite with the presence of Cu but there is a slight shifting.[32–36]

Figure 1 presents the FT-IR spectra of pure nanocomposites as well as nanocomposites with copper. The wave number of the spectra was

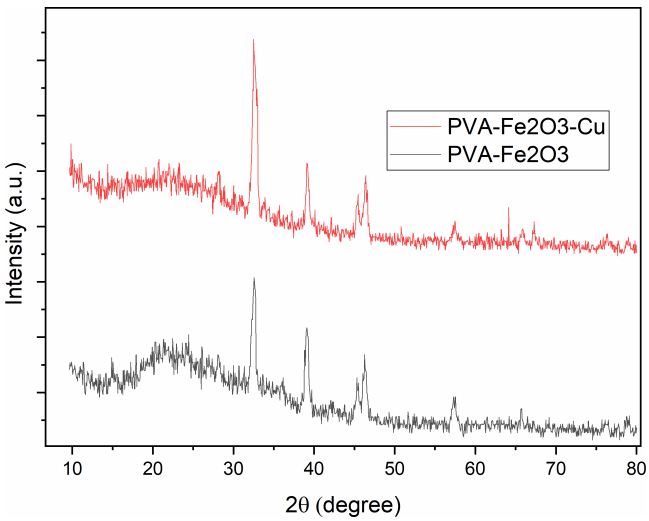


Fig. 1. XRD Curve of prepared materials.

modified from 4000 $cm^{-1}$ down to 500 $cm^{-1}$, as can be seen from Fig. 2. The O–H bond stretching is accountable for the absorbance band at 3270 $cm^{-1}$, whereas the C=O stretching is responsible for the absorption band in the range of 1639–2858 $cm^{-1}$.[37] Metal oxide (M–O) stretching is responsible for the sharp peak that may be found at 577 $cm^{-1}$. The existence of M–O stretching is irrefutable evidence that $Fe_2O_3$ NPs have been formed.[37] After adding Cu, this peak was shifted down to 556 $cm^{-1}$.

The surface properties and morphology of prepared composites have been examined via the scanning electron microscope before and after doping with Cu ions. Figure 3 shows the SEM graphs at different magnification scales where Figs. 3(a)–3(c) represent the morphology of PVA–$Fe_2O_3$ before adding Cu and Figs. 3(e)–3(g) represent the morphology of nanocomposite after adding Cu. From the graphs in Fig. 3, the shape of nanostructures is spherical and capped well with PVA polymer for both composites but the nanocomposite after adding Cu became more dense with a less homogenous structure. New particles with darker color appeared after doping which maybe represents Cu NPs formed during the preparation process.

The optical transmission spectra of prepared composites before and after adding Cu ions were tested to study the effect of Cu ions on transparency of materials. Figure 4 displays the spectra of transmission of nanocomposites. Before the doping process, the nanocomposite material has very high transmission in the range of wavelengths (550–800 nm) where it reached 83% but the transmission faced a dropping to 53% at the same wavelength

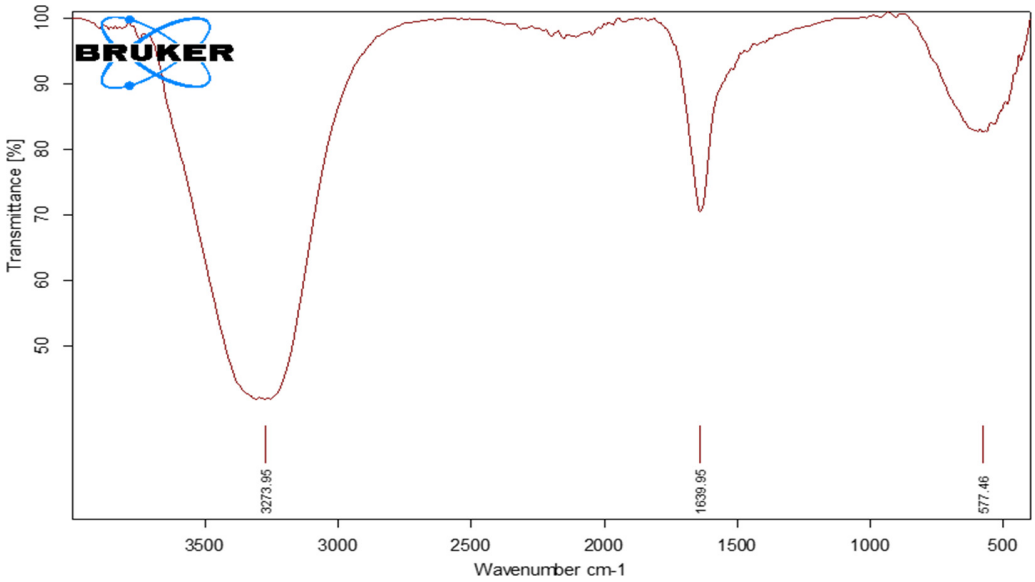


(a)

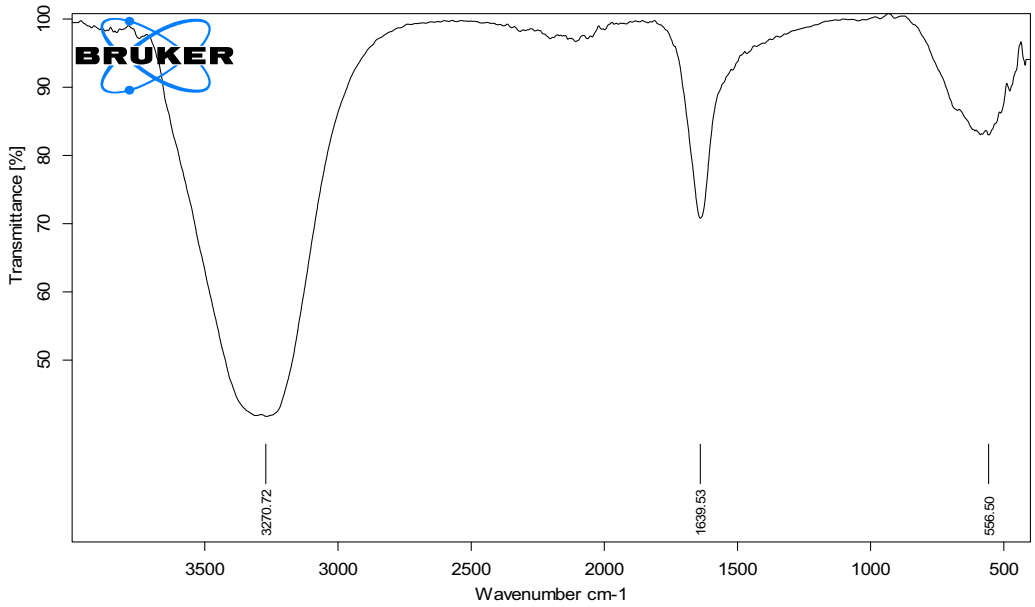


(b)

Fig. 2. FTIR bands of (a) $Fe_2O_3$–PVA and (b) $Fe_2O_3$:Cu–PVA.

range after inserting the Cu ions in the composite structure.

Figure 5 depicts the Uv–Vis absorbance of the produced nanocomposites, which were analyzed in the range of wavelength limited between 400 nm and 900 nm. The absorbance bands of PVA–$Fe_2O_3$ and PVA–$Fe_2O_3$–Cu nanocomposite demonstrate that all absorption curves exhibit a significant absorption in the area of 450–550 nm.

Figure 6 displays the band gap of PVA–$Fe_2O_3$ and PVA–$Fe_2O_3$–Cu. The PVA–$Fe_2O_3$ energy bandgap is around 2.16 eV, but it lowers when composite with Cu, becoming equivalent to 2.06 eV. The majority of the responsibility for shiftting in bandgap rests with Cu.[38] Because the PVA–$Fe_2O_3$–Cu molecule's absorption range was greatly expanded toward longer wavelengths, we are now able to harvest a greater quantity of visible light and search for potential applications in the fields of energy and the environment.

Iron oxide NPs consider very efficient materials in anticancer and other medical applications.[39]

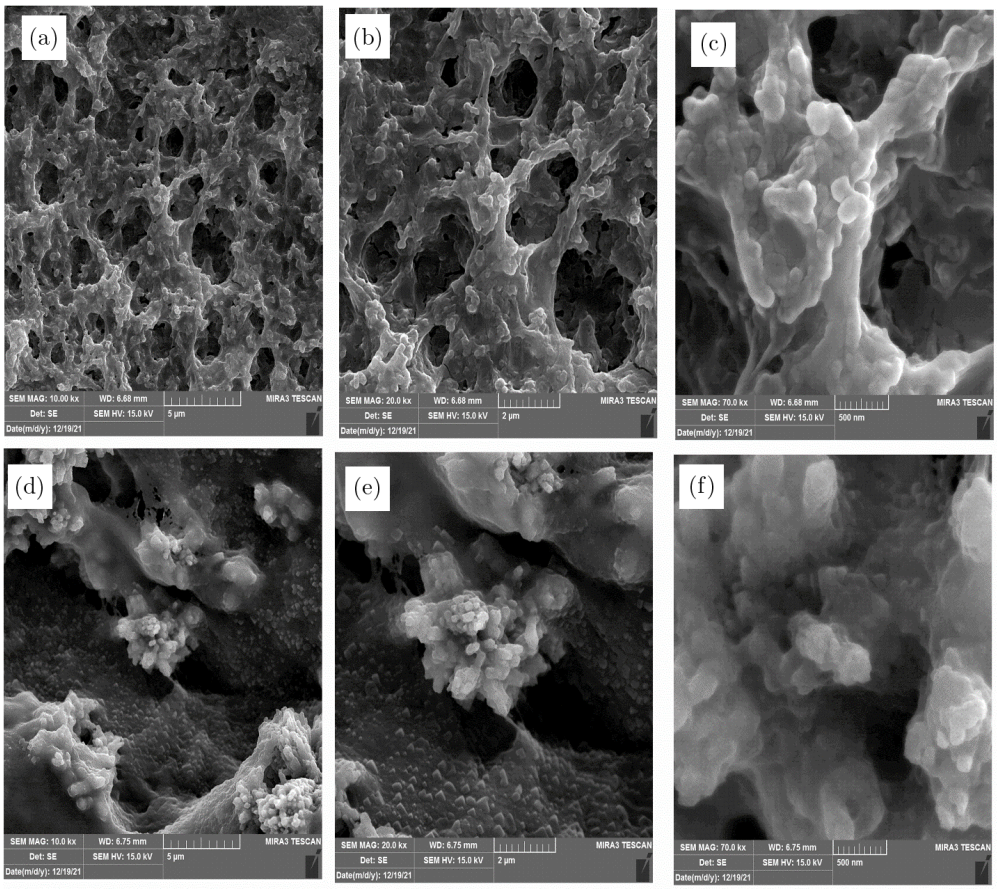


Fig. 3. FESEM images of (a)–(c) PVA–$Fe_2O_3$ and (d)–(f) PVA–$Fe_2O_3$–Cu.

The activity of prepared materials as anticancer materials has been tested by applying the MTT assay method on MSF-7 cells line, this method is a very popular and efficient method to test the activity of nanomaterials on tumor cells.[40] The MTT assay is shown in Fig. 7.

Holographic representation of the relationship between the concentration of nanocomposite and survival cell is shown in Fig. 8. It is possible to draw the following conclusion from the figure: the number of surviving cells will decrease as the concentration of nanocomposite increases. The nanocomposites after doping were more effective on tumor cells.

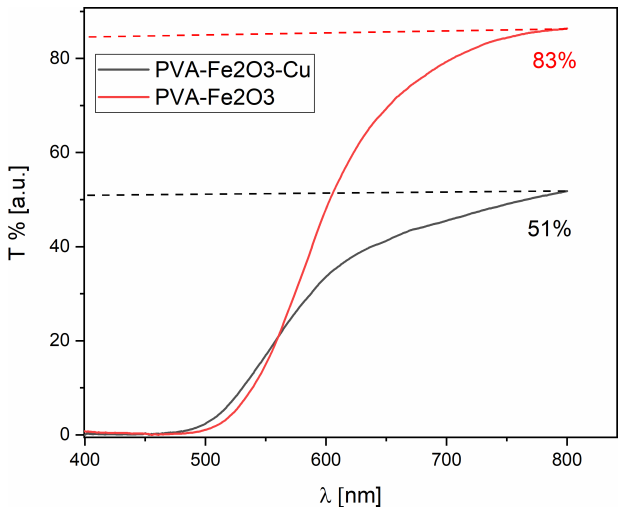


Fig. 4. UV–Vis transmission spectra of nanocomposites.

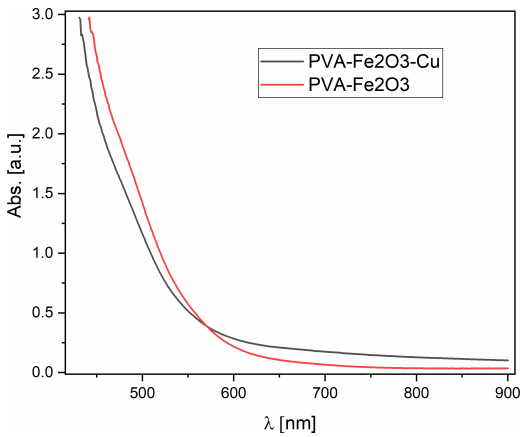


Fig. 5. UV–Vis absorbance spectrum of nanocomposites.

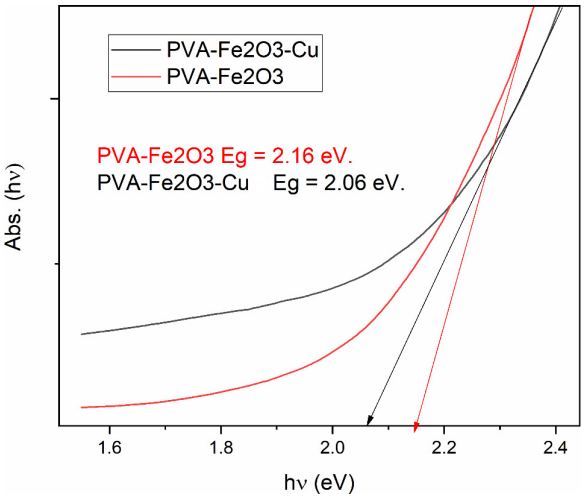


Fig. 6. Optical band gaps of nanocomposites.

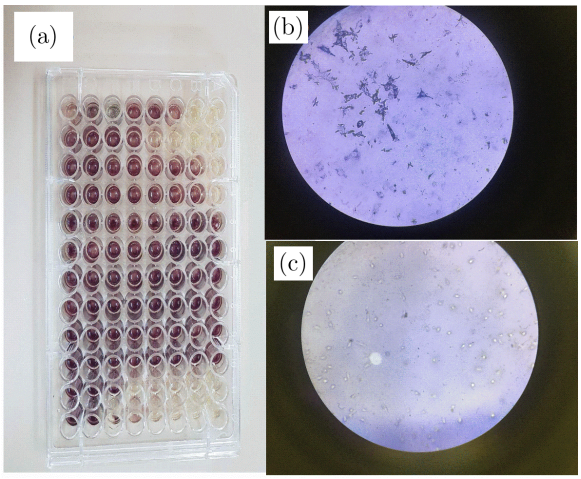


Fig. 7. (a) MTT assey image of MCF-7 cell line, (b) inverted microscoping image of MCF-7 cell before adding nanocomposite and (c) inverted microscoping image of MCF-7 cell after adding nanocomposite.

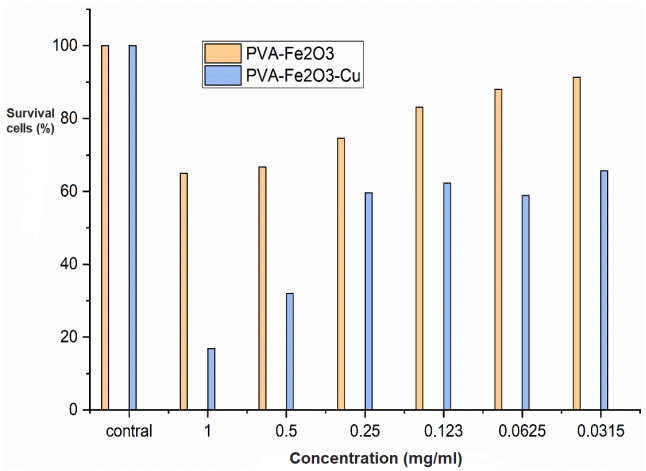


Fig. 8. Holographic representation of the relationship between the concentration of nanocomposite and survival cell.

## 4. Conclusions

(1) PVA–$Fe_2O_3$–Cu nanocomposites have been successfully prepared by the chemical method approach.
(2) The impacts of adding Cu ions were examined on some main physical properties of nanocomposites.
(3) The crystal structure of prepared nanocomposites remains the same before and after Cu ions adding.
(4) The morphology and homogeneity of composites changed after adding Cu ions and the material became more rough and dense.
(5) The transmission of composites was reduced after adding Cu ions.
(6) The energy gap became smaller after adding Cu ions.
(7) The anticancer activity was tested on tumor cells by using the MTT assay method and it can be concluded that the prepared composites have good killing activity for tumor cells.

## References

1. S. Nallusamy and A. Karthikeyan, *J. Nano Res.* **49**, 1 (2017).
2. S. Nallusamy and A. Manoj Babu, *J. Nano Res.* **37**, 58 (2016).
3. K. A. Mohammed, A. S. Al-Kabbi and K. M. Zidan, *AIP Conf. Proc.* **2144**, 030009 (2019).
4. P. B. E. Kedi *et al.*, *Int. J. Nanomed.* **13**, 8537 (2018).
5. S. Nallusamy, *J. Nano Res.* **40**, 105 (2016).
6. I. Ijaz, E. Gilani, A. Nazir and A. Bukhari, *Green Chem. Lett. Rev.* **13**, 223 (2020).
7. G. Bupesh, E. Manikandan, K. Thanigaiarul, S. Magesh and V. Senthilkumar, *J. Nanomed. Nanotechnol* **7**, 355 (2016).
8. T. Zhang *et al.*, *Nanomaterials* **7**, 220 (2017).
9. B. H. Kim, M. J. Hackett, J. Park and T. Hyeon, *Chem. Mater.* **26**, 59 (2014).
10. K. A. Mohammed *et al.*, *Mater. Today: Proc.* **56**, 2010 (2022).
11. S. M. Cromer Berman, P. Walczak and J. W. Bulte, *Wiley Interdiscip. Rev. Nanomed. Nanobiotechnol.* **3**, 343 (2011).
12. H. Hofmann *et al.*, *Nanostructured Materials* (Springer-Verlag Wien, 2002).
13. Z. Luo and H. Du, *Stem Cell Rev. Rep.* **16**, 675 (2020).
14. D. Havenga *et al.*, *Sci. Rep.* **12**, 2259 (2022).
15. M. Geppert and M. Himly, *Front. Immunol.* **12**, 2366 (2021).

16. S. Kumar, M. Kumar and A. Singh, *Contempor. Phys.* **62**, 144 (2021).
17. Y. Liu, L. Yu, Y. Hu, C. Guo, F. Zhang and X. W. D. Lou, *Nanoscale* **4**, 183 (2012).
18. J. Lian, X. Duan, J. Ma, P. Peng, T. Kim and W. Zheng, *ACS Nano* **3**, 3749 (2009).
19. S. Elbasuney, A. Elsaidy, M. Kassem and H. Tantawy, *J. Inorg. Organometall. Polym. Mater.* **28**, 1718 (2018).
20. K. Ssekatawa, D. K. Byarugaba, E. M. Wampande, T. N. Moja, E. Nxumalo, *Sci. Rep.* **11**, 1 (2021).
21. M. G. Zaky, A. Elbeih and T. Elshenawy, *Cent. Eur. J. Energ. Mater.* **18**, 63 (2021).
22. J. Fang, J. He, E. Y. Shin, D. Grimm, C. J. O'Connor and M. J. Jun, *MRS Online Proc. Libr.* **774**, 1 (2003).
23. S. M. S. Hosseini and M. S. Dehaj, *J. Taiwan Inst. Chem. Eng.* **135**, 104381 (2022).
24. A. Shylaja, S. Manikandan, K. S. Suganthi and K. S. Rajan, *J. Nanosci. Nanotechnol.* **15**, 1653 (2015).
25. A. T. Khalil, M. Ovais, I. Ullah, M. Ali, Z. K. Shinwari and M. Maaza, *Green Chem. Lett. Rev.* **10**, 186 (2017).
26. S. O. Aisida, P. A. Akpa, I. Ahmad, T. K. Zhao, M. Maaza and F. I. Ezema, *Eur. Polym. J.* **122**, 109371 (2020).
27. E. H. Al-Tememe, H. M. A. A. Algalal, A. A. F. Abodood, K. A. Mohammed, E. J. Khamees, R. S. Zabibah and A. S. Abed, *Int. J. Nanosci.* **21**, 2250018 (2022).
28. H. Chen, F. Liu, Z. Lei, L. Ma and Z. Wang, *RSC Adv.* **5**, 84980 (2015).
29. S. A. Hammood *et al.*, *Int. J. Nanosci.* **21**, 2250030 (2022).
30. R. P. Lefojane *et al.*, *Sci. Rep.* **11**, 1 (2021).
31. A. Sani *et al.*, *J. Biomole. Struct. Dyn.* **39**, 4133 (2021).
32. A. C. Nwanya, M. M. Ndipingwi, C. O. Ikpo, F. I. Ezema, E. I. Iwuoha and M. Maaza, *J. Electroanal. Chem.* **858**, 113809 (2020).
33. R. Hatel, M. Khenfouch, M. Baitoul and M. Maaza, *Appl. Phys. A* **120**, 1069 (2015).
34. X. Fuku *et al.*, *AIP Conf. Proc.* **1962**, 040006 (2018).
35. M. G. Tsegay, H. G. Gebretinsae, G. G. Welegergs, M. Maaza and Z. Y. Nuru, *Solar Energy* **236**, 308 (2022).
36. D. Hassan, A. T. Khalil, J. Saleem, A. Diallo, S. Khamlich, Z. K. Shinwari and M. Maaza, *Artif. Cells Nanomed. Biotechnol.* **46**, 693 (2018).
37. V. Parthasarathy, J. Selvi, Senthil P. Kumar, R. Anbarasan and S. Mahalakshmi, *Polym. Bull.* **78**, 2191 (2021).
38. O. A. Chichan, S. H. Nowfal, H. N. Abd, K. H. Abass, N. F. Habubi and S. S. Chiad, **7**, 1960 (2022).
39. N. Ditlopo, *et al.*, *Sci. Rep.* **12**, 3468 (2022).
40. A. T. Khalil, M. Ovais, I. Ullah, M. Ali, S. A. Jan, Z. K. Shinwari and M. Maaza, *Arab. J. Chem.* **13**, 916 (2020).